Journal of Thermal Analysis and Calorimetry, Vol. 78 (2004) 1043–1055

INFLUENCE OF THE PARTICLE-SIZE REDUCTION BY ULTRASOUND TREATMENT ON THE DEHYDROXYLATION PROCESS OF KAOLINITES

F. Franco[1*], *L. A. Pérez-Maqueda*[2] *and J. L. Pérez-Rodríguez*[2]

[1]Departamento de Química Inorgánica, Cristalografía y Mineralogía, Facultad de Ciencias, Campus de Teatinos, Universidad de Málaga, 29071 Málaga, Spain
[2]Instituto de Ciencia de Materiales de Sevilla, Centro Mixto C.S.I.C.-Universidad de Sevilla, C/Américo Vespucio s/n, Isla de la Cartuja, 41092 Sevilla, Spain

(Received May 14, 2004)

Abstract

Kaolinites from well-known sources (KGa-1 and KGa-2) were used to study the influence of the particle-size reduction on the dehydroxylation process. Size reduction of particles was obtained by ultrasound treatment to avoid the effect of the progressive amorphization of the structure, which takes place with the traditional grinding treatment.

The particle-size reduction causes an increase of the mass loss between 140 and 390ºC attributed to the loss of the hydroxyl groups exposed on the external surface of kaolinite; a shift to lower temperatures of the endothermic effect related with the mass loss between 390 and 600ºC; and a shift of the end of dehydroxylation to lower temperatures. The first modification can be explained by an increase of the number of hydroxyls exposed on the external surface of kaolinite which is proportional to the new surface generated in the particle reduction process, whereas the shift of the dehydroxylation to lower temperatures is related to the reduction of the dimensions of the particles which favour the diffusion controlled mechanisms.

Comparing between the DTA curves to the TG curves of the studied samples shows that the observed modifications in the thermal properties induced by the particle-size reduction are greater for the low-defect kaolinite. The intensity of these modifications depends on the effectiveness of the ultrasound treatment.

Keywords: kaolinite, mass loss, particle-size reduction, sonication, structural disorder, thermal analysis

Introduction

Kaolinite finds almost innumerable applications, and the diversity of uses is still increasing. These applications include uses in the fabrication of paper as filler or coating, extender in paints and inks, filler in rubber and in plastic, ceramic raw material,

* Author for correspondence: E-mail: ffranco@uma.es

1388–6150/2004/ $ 20.00

Akadémiai Kiadó, Budapest
Kluwer Academic Publishers, Dordrecht

fiberglass, cracking catalysts, cosmetic, medicines, etc. [1, 2]. In all applications, kaolinite has a function and is not just an inert component of the system. Properties of kaolinite, particularly important for industrial applications, are particle-size distribution, crystallinity, surface area and whiteness [2].

In addition to the traditional applications, new uses are found as the physical properties of kaolinite are modified with the development of new treatments. Some of these new applications are closely related to the particle-size of the mineral, which finally influences the surface reactivity of kaolinite.

Particle-size reduction has been traditionally obtained by grinding (either wet or dry) [3–9]. This treatment increases the specific surface area of kaolinite within the first minutes, but they produce undesirable effects, like the total degradation of the crystal structure and the formation of hard aggregates, which causes a dramatic decrease of the ground kaolinite surface area [10]. The grinding treatments also have a clear effect on the dehydroxylation of kaolinite. Thus the DTA endothermic effect related with the dehydroxylation process shifts to lower temperatures (from 565 to 490ºC) as the time of treatment increases and disappears completely, after 120 min of grinding, when kaolinite was completely transformed into an amorphous material [10].

Very recently, it has been reported the use of sonication, as alternative to grinding, for particle-size reduction of clay minerals. For example, in the case of the sonication of vermiculite [11, 12] sonication produces not only a delamination effect but also a breaking of layers in the other directions, while the crystalline character is retained. Thus, crystalline nanometric and submicron-sized vermiculite flakes were prepared from a natural macroscopic vermiculite sample by a sonication procedure. Similar results were obtained in the sonication of micas. Pérez-Maqueda *et al.* [13] described the conditions for the preparation of crystalline micron and submicron-sized muscovite and biotite. In this sense, Franco *et al.* [14] reported the effect of ultrasound on the structure of a well ordered kaolinite. Thermal analysis is widely used in the study of properties of minerals of the kaolin group (e.g. [15–17]). In the present work we are going to show that sonication treatment produces significant delamination and particle-size reduction along the *b* axis, whereas the crystalline structure of kaolinite is not damaged.

The effect of the particle-size reduction, obtained by sonication treatments on the dehydroxylation of clay minerals have not been extensively studied. The aim of this work is to examine the effect of the particle-size reduction by ultrasound treatment on the thermal behaviour of both low-defect (KGa-1) and high-defect (KGa-2) reference kaolinite samples (Georgia kaolinite Co.).

Experimental

Materials

The starting materials used for the present study were low-defect and high-defect Georgia kaolinite (KGa-1 and KGa-2, previously referred to as ‘well-crystallized’ and ‘poorly-crystallized’, respectively), supplied by the Clay Minerals Society, Source

Clays Minerals Repository, University of Missouri, Columbia, MO, USA. These two kaolinite powders, both from Georgia, have been extensively characterized [17–19].

Methods

Ultrasonic treatments were performed with a Misonic ultrasonic liquid processor of 600 W output with a 20 kHz converter and tapped titanium disruptor horn of 12.7 mm in diameter that produces a double (peak to peak) amplitude of the radiating face of the tip of 120 μm. The horn tip was dipped into a cylindrical jacketed cooling cell of 5 cm in internal diameter, where 1.5 g of kaolinite were mixed with 40 mL of freshly deionized water. The dispersions were sonicated for periods ranging from 5 to 60 h. The temperature reactor was kept constant at 20ºC during the entire treatment by means of a cooling recirculator. After treatment, samples were lyophilised to remove the water of the suspension.

Brunauer–Emmet–Teller (BET) specific surface areas (*ssa*) were obtained with an automatic system (Model No. 2200 A, Micromeritics Instrument Corp., Norcross, GA), using nitrogen gas as an adsorbate at liquid nitrogen temperature. The samples previously were outgassed at 140ºC for 2 h. The equivalent spherical diameter (*esd*) was calculated from the *ssa* by means of the expression

$$esd=[6/(\sigma S)]\times 1000$$

where *esd* is the equivalent spherical diameter (nm), σ is the density of the material (2.64 g cm^{-3}), and *S* is the *ssa* (m^2 g^{-1}) determined by BET.

X-ray diffraction patterns were obtained using a Siemens D-5000 diffractometer. The XRD patterns were obtained using CuK_α radiation, at 40 kV and 35 mA, and a step size of 0.02º 2θ at a counting time of 3 s. Measurements were performed on randomly oriented powder preparations. Defects in kaolinite were measured using the Hinckley index (HI) [20]. The apparent coherent scattering thickness of the kaolinite crystals was calculated along the c^*-axis, using the 002 reflection (CS_{002}) and along the *b* axis, using the 060 reflection (CS_{060}) according to the Scherrer formula [21]. The width of the peaks corresponding to the 002 and 060 reflections was calculated using the Peakfit software from Jandel Scientific.

Thermogravimetric analysis (TG) and differential thermal analysis (DTA) were carried out simultaneously in an automatic thermal analyser system (Seiko, TG/DTA 6300). Samples of about 40 mg were packed loosely into a platinum holder and were thermally treated at a heating rate of 10ºC min^{-1} in Ar flow (400 cc min^{-1}).

Results and discussion

Specific surface area

Figure 1 shows the specific surface area (*ssa*) variation for the studied kaolinites (KGa-1 and KGa-2) as a function of the sonication time. The obtained values of *ssa* are also presented in Table 1. This figure clearly reveals that sonication produces a

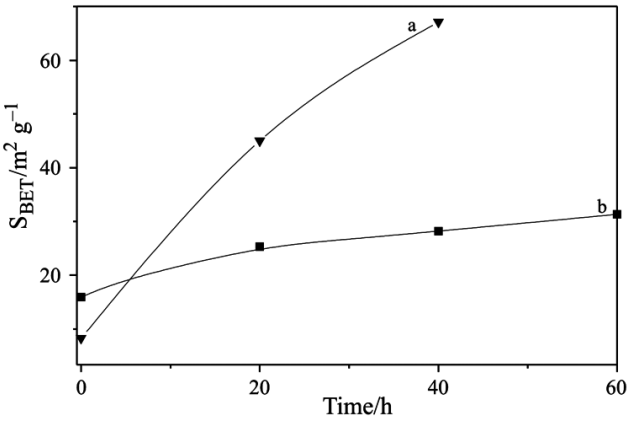

Fig. 1 Evolution of the specific surface area: a – KGa-1; b – KGa-2

remarkable *ssa* increase in the KGa-1 sample (Fig. 1a) with the treatment time. This increase is continuous and no evidences of decreasing due to the formation of hard aggregates are observed even after 40 h of treatment. For KGa-1 sample, *ssa* increases from 8.5 to 45 $m^2\ g^{-1}$ after 20 h of treatment. When the sonication time increases beyond 20 h, the *ssa* also increases reaching 67 $m^2\ g^{-1}$ at 40 h. These results contrast those observed in the traditional grinding treatment [10].

The variation of the *ssa* of KGa-2 sample *vs.* time of treatment is shown in Fig. 1b. The *ssa* of the untreated KGa-2 (16 $m^2\ g^{-1}$) is higher than that of the untreated KGa-1 (8.5 $m^2\ g^{-1}$). Nevertheless, the *ssa* increments obtained after sonication treatments are notably smaller than that obtained for KGa-1 sample. After 20 h of sonication the *ssa* of KGa-2 increases from 16 to 25 $m^2\ g^{-1}$. The *ssa* continues increasing with the time of treatment and at 60 h the *ssa* is 31 $m^2\ g^{-1}$. These data reveal that the obtained values of the *ssa* after sonication treatment are strongly influenced by the characteristic features of the starting kaolinites.

The results obtained with sonication treatments are notably different of those obtained by Sánchez-Soto *et al*. [10] in the grinding treatment of the same kaolinite samples. They observed a strong decrease of the *ssa* of the ground kaolinites after 20 min of grinding because the kaolinite particles became agglomerated. In our case, when the *ssa* is enhanced with an ultrasound treatment, this increase is continuous with the time of treatment, and it is possible to reach *ssa* values notably higher than those observed for the untreated kaolinites. Franco *et al*. [22] studied by LALLS (Low-angle laser light scattering) the particle-size distribution of the sonicated KGa-1 samples. They showed that, after sonication periods of 20 h, the ultrasound treatment reduces the size of the particles higher than 1 μm and increase notably the proportion of the smallest particles (0.5 μm), without the formation of hard aggregates. Nevertheless, at the longest sonication time (40 h) a very small proportion of particles become agglomerated. Apparently, the strong agitation to which the particles are subjected is greater than the surface energy created with the impacts and it prevents the formation of the hard aggregates observed after grinding treatments [14, 22].

The values of the equivalent spherical diameters (*esd*) of the studied samples are also included in Table 1. Although, these values do not pretend to give absolute values of particle size due to the anisotropic shape of the clays, they give information about the evolution of the particle size with the treatment. These values indicate that there is a sharp decrease in the particle size for the sonicated samples. For the untreated kaolinite the *esd* has a value of 266 nm. After 20 h treatment the *esd* of KGa-1 decreases to 50 nm, and becomes 34 nm after 40 h treatment. On the other hand, the decrease of the *esd* of KGa-2 is notably lower. The *esd* of the untreated KGa-2 (142 nm) decreases to 73 nm after 60 h sonication.

Table 1 Specific surface areas, equivalent spherical diameter and crystalline data of the starting kaolinite and of treated kaolinites

Sample	*t*/h	*ssa*/m^2 g^{-1}	*esd*/nm	CS_{002}/nm	CS_{060}/nm	H.I.
KGa-1*	0	8	266	42.4	26.1	1.19
	20	45	50	35.3	24.8	0.60
	40	67	34	35.1	22.9	0.53
KGa-2*	0	16	142	27.4	23.6	0.12
	20	25	91	27.0	23.5	0.13
	40	28	81	26.4	22.6	0.11
	60	31	73	24.2	22.4	0.12

*Starting kaolinite. *t*=time of treatment in hours; *ssa*= specific surface area; CS_{002} and CS_{060}=apparent coherent scattering thickness measured using the Scherrer formula on 002 and 060 reflections; H.I.=Hinckley index [17].

X-ray diffraction study

The method used to measure the particle-size (*esd*) assumed that particles are spherical. Considering that kaolinite is a lamellar silicate, it is of interest to obtain information on the dimension in different crystallographic directions. Table 1 includes the crystallite size of the untreated kaolinites (KGa-1 and KGa-2) and of the sonicated samples as calculated by the Scherrer broadening method using the 002 and 060 reflections (12.38 and 62.31º 2θ, respectively) [21]. The 002 reflection is a basal one and may be used for a direct estimation of the particle thickness. Nevertheless, we have to take into account that this size is related to microdomains of coherent scattering and not to agglomerates.

The value of the coherent diffraction thickness along the c^*-axis, of the KGa-1 subjected to ultrasound decreases from 42.4 to 35.3 nm after 20 h and to 35.1 nm after 40 h of sonication (Table 1). In the case of KGa-2, the coherent diffraction thickness along the c^*-axis decreases from 27.4 nm to 27.0, 26.4 and 24.2 nm after 20, 40 and 60 h of sonication, respectively (Table 1). It is interesting to note, that the decreasing of the particle thickness of the KGa-1 sample along the c^*-axis, after 40 h of sonication treatment, (a decrease of 17.2% of the original value) is notably higher than that of the KGa-2 after a similar time treatment (3.7% of the original value).

The ultrasound treatment also causes the progressive broadening of the 060 reflection indicating that the dimension of kaolinite crystals along the *b* axis also decreases with the time of ultrasound treatment (Table 1), due to the transverse breakage of the kaolinite flakes. The coherent scattering thickness along the *b* axis decreases from 26.1 to 22.9 nm in 40 h treatment (a decrease of 12.26% of the original value). On the contrary, the decrease of the particle-size along the *b* axis of KGa-2 is notably lower. At 60 h treatment the coherent scattering thickness along the *b* axis of KGa-2 decreases by about 5% of the original value.

Figure 2a shows the XRD pattern of the starting KGa-1 between 10 and 42º 2θ. The reflections 02*l*, 11*l* of the KGa-1 sample, are narrow and intense, indicating that this kaolinite is a well crystallized kaolinite. Important modifications of the 02*l*, 11*l* reflections of the KGa-1 sample are observed with the time of treatment (Fig. 2a). The Hinckley index (H.I.) [20] decreases from 1.19 to 0.60 after 20 h of treatment. This result indicates that great increase in translation defects takes place in the

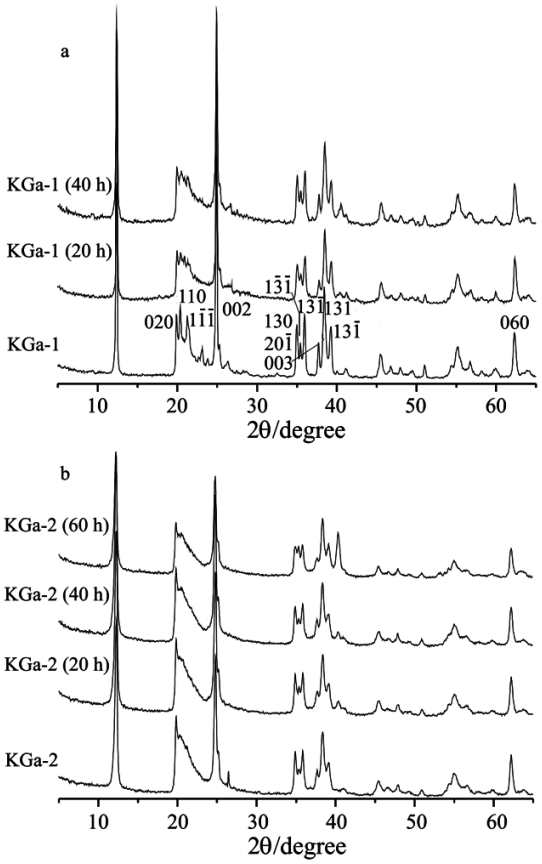

Fig. 2 X-ray diffraction patterns of the a – KGa-1and b – KGa-2 samples after increasing time of treatment

sonication of KGa-1 during this time of treatment. On the contrary, between 20 and 40 h of sonication, the increase in translation defect is sensibly smaller (H.I. varies from 0.60 to 0.53).

On the other hand, reflections 11*l* of the untreated KGa-2 sample (Fig. 2b) are broad and their overlapping results in a wide band, extending between 19 and 24º 2θ, attached to the right side of the 020 reflection. These XRD profiles indicate that KGa-2 is a high defected kaolinite. The values of H.I. (0.12 for untreated and treated KGa-2 samples) indicate that the sonication treatment on KGa-2 does not increase the proportion of the structural defects.

The XRD patterns of the treated samples indicate that the structural changes induced by the sonication treatment depend on the characteristic features of the starting kaolinite. The well ordered kaolinites, such as KGa-1, are more sensitive to sonication treatments as shown the higher increasing of structural disorder and the decreasing of the particle thickness along the c^*-axis, whereas the disordered kaolinites, such as KGa-2, are more resistant. However, contrarily to that observed previously in the grinding treatment, where a total degradation of the kaolinite structure was observed [10], both kaolinite samples (KGa-1 and KGa-2) remain crystalline even after 60 h of sonication as indicated by the persistence of the 13*l* reflections.

Thermal analysis

The TG curves of untreated kaolinites (KGa-1 and KGa-2) and of sonicated samples are shown in Fig. 3. The TG curve of untreated KGa-1 (Fig. 3a) shows that a continuous heating rate originates a slight mass loss below 140ºC, associated with the loss of the loosely bonded adsorbed water on the particle surface. Between 140 and 230ºC the TG curve shows that the mass remains constant. A slight mass loss between 230

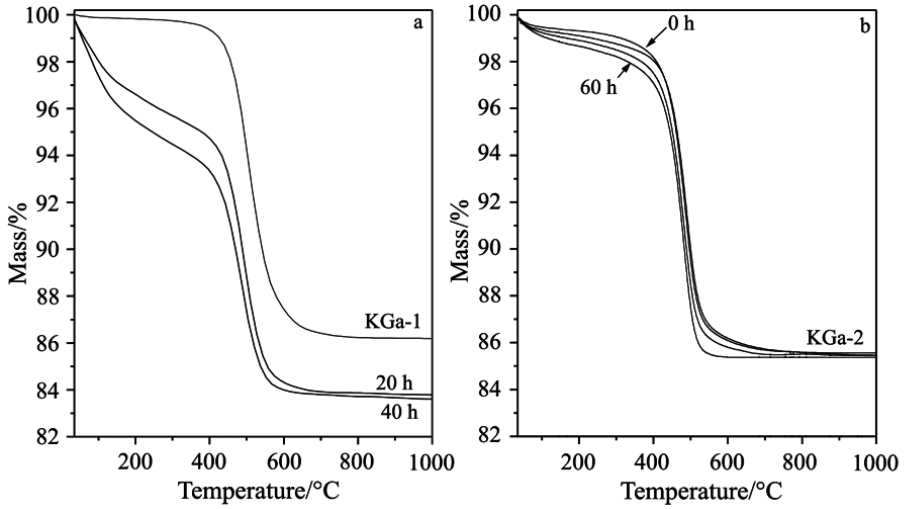

Fig. 3 TG curves of a – KGa-1 and b – KGa-2 samples (40 mg) before and after different times of ultrasound treatment at 20 h intervals

and 440ºC is followed by a change in the slope of the TG curve, indicating a faster mass loss from 440 to 580ºC. After this temperature the mass loss rate decreases and stops at 835ºC. These three stages of mass loss are associated with the dehydroxylation process. The different rates of mass loss, between 230 and 835ºC, indicate that the dehydroxylation of KGa-1 occurs in several stages. The mass losses in the several stages are shown in Table 2.

Table 2 Mass loss (%) in the several thermal processes obtained from the TG curves of the starting kaolinite and of treated kaolinites

Sample	*t*/h	Desorption of adsorbed water/%	First stage of dehydroxylation/%	Second stage of dehydroxylation/%
KGa-1	0	0.1	0.14	13.57
	20	2.61	3.74	9.72
	40	3.95	4.35	9.44
KGa-2	0	0.29	1.75	12.25
	20	0.35	2.01	11.98
	40	0.51	2.14	11.67
	60	0.67	2.63	11.37

The TG curves of the sonicated KGa-1 samples (Fig. 3a) show greater mass losses below 140ºC compared with that observed in the TG curve of untreated kaolinite (Table 2). These results suggest an increase of the amount of adsorbed water proportional to the increase of surface area in the sonicated kaolinites [14]. From this temperature, mass loss continues up to 717 and 655ºC in the KGa-1 samples sonicated 20 and 40 h, respectively. Thus, the particle-size reduction is progressively reducing the temperature of the end of the dehydroxylation process. Moreover, as the sonication time increases the different stages of mass loss between 140 and 835ºC are better defined due to the increasing of mass loss in the first stage of dehydroxylation. When sonication time increases, the mass loss in this first stage increases whereas the mass loss in the second stage decreases.

The stages of mass loss, described above, are observed as maxima in the DTG curves (Fig. 4a). The first stage, attributed to the loss of adsorbed water is centred at 54ºC. The second stage, attributed to the first stage of dehydroxylation, is not well defined in the DTG curve and it appears as an increase of the background of the DTG curve between 140 and 390ºC. The third mass loss stage, attributed to the second stage of dehydroxylation, is observed as a well-defined peak, which decreases with sonication time as the background between 140 and 390ºC increases. At the same time the maximum shifts from 506 to 482ºC, after 40 h of sonication treatment. On the other hand, a shoulder appears on the high temperature side of the peak at 506ºC in the DTG curve of the untreated KGa-1 (Fig. 4a), which is not present in the DTG curve of the sonicated samples. With the results presented in this work it is difficult to explain the existence of this shoulder. It can be associated with the elimination of

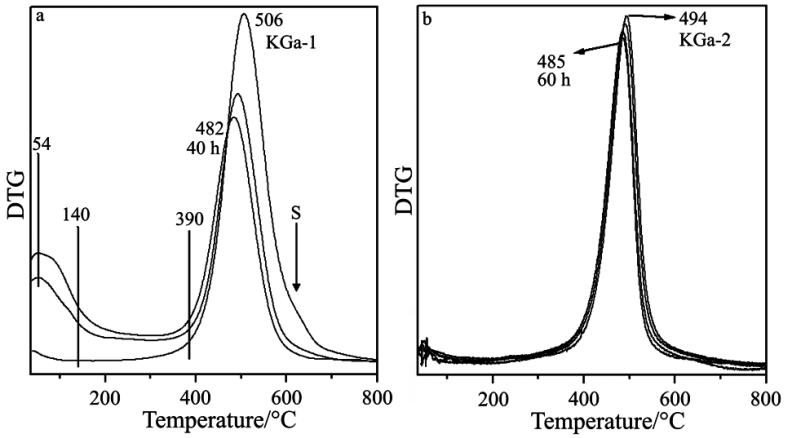

Fig. 4 DTG curves of a – KGa-1 and b – KGa-2 samples (40 mg) before and after different times of ultrasound treatment at 20 h intervals

ions trapped in the metakaolinite framework of the larger particle-size fraction of KGa-1 after the dehydroxylation.

The DTA curve of untreated KGa-1 (Fig. 5a) shows a weak endothermic effect centred at 100ºC associated with the loss of adsorbed water, whereas the dehydroxylation process originates an endothermic effect (between 400 and 650ºC) centred at 506ºC. At higher temperatures, an intense exothermic effect is also observed (between 961 and 1004ºC) at 987ºC, which is related with the formation of either mullite nuclei or a phase with a spinel-type structure, γ-alumina or a cubic phase or both [23, 24].

The variations of the DTA curve of the KGa-1 samples (Fig. 5a) after sonication are similar to that described for the DTG curves. The DTA curves of sonicated KGa-1

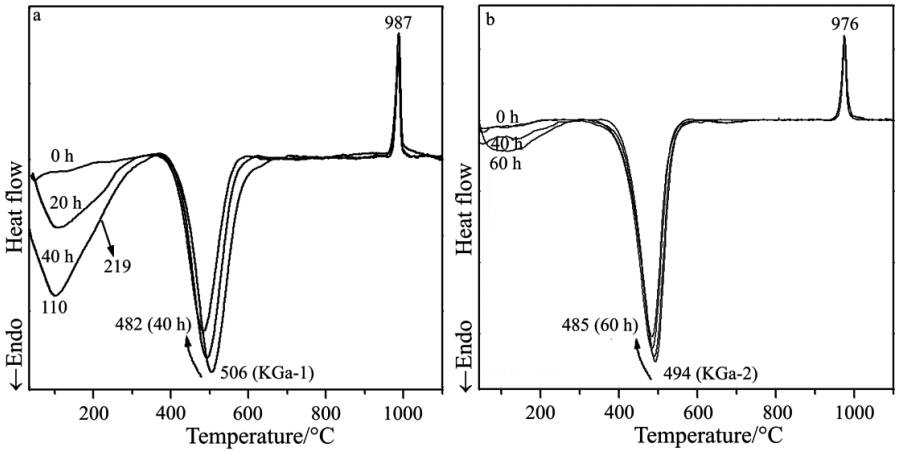

Fig. 5 DTA curves of a – KGa-1 and b – KGa-2 samples (40 mg) before and after different times of ultrasound treatment at 20 h intervals

samples show an increase in the endothermic centred at 110ºC with the time of treatment. This endothermic effect is complex and appears to be represented, at least, by two maxima at 110 and 219ºC. According to the mass losses in this temperature range, the endothermic effect centred at 110ºC is attributed to the loss of adsorbed water whereas the endothermic effect centred at 219ºC can be attributed to the loss of protonated hydroxyls formed during the sonication treatment due to prototropy and to hydroxyl groups located on the external surface of the particle. Similar to the DTG curves, the DTA curves of sonicated KGa-1 samples show that the endothermic effect shifts to lower temperatures (from 506 to 482ºC after 40 h of sonication) and decreases in intensity as the endothermic effect centred at 219ºC increases. According to Franco *et al*. [14] and Dion *et al*. [25], this shift may be explained in terms of particle-size reduction along the *c*-axis and increasing of structural disorder induced by the sonication treatment. On the contrary, the temperature of the exothermic effect at 987ºC is not affected by the sonication treatment (Fig. 5a).

The DTA-TG curves of untreated KGa-2 present some differences with that of KGa-1, which have to be taken into account. First, the TG curve of untreated KGa-2 (Fig. 3b, Table 2) shows a higher mass loss in the first stage of dehydroxylation than the observed in the TG curve of untreated KGa-1. This suggests a higher number of hydroxyl groups exposed on the external surface of untreated KGa-2. In fact, there is a strong correlation between the number of exposed hydroxyls, the specific surface area and the mass loss in the first stage of dehydroxylation. Second, the endothermic effect of the dehydroxylation of untreated KGa-2 (Fig. 5b) appears at lower temperatures (494ºC) than the observed for the untreated KGa-1 (506ºC) (Fig. 5a). In this case, these differences can be attributed to the smaller particle size and the higher structural disorder of the KGa-2 sample. These two parameters, as pointed out by Dion *et al.* [25], affect the temperature of dehydroxylation.

The TG curves of sonicated KGa-2 samples (Fig. 3b, Table 2) also show an increase of the mass loss in the temperature range between 140 and 400ºC with the sonication time, as occurred with the KGa-1 sample. Nevertheless, the increase of the mass loss in this stage is notably lower than that generated with the sonication of KGa-1 samples. These results correlate with the lower increase in specific surface area obtained in the KGa-2 sample.

The mass loss of the second stage of the dehydroxylation process, in KGa-2 samples, appears as a well-defined band in the DTG curve (Fig. 4b), which is progressively shifted to lower temperatures as the sonication time increases. Nevertheless, the shift of the maximum of this peak, after 60 h sonication (9ºC), is smaller than that observed for the KGa-1 sample after 40 h treatment (24ºC).

The DTA curves of the sonicated KGa-2 samples show that the endothermic centred at 494ºC shifts to 485ºC after 60 h of sonication treatment. This shift is also smaller than that observed in the sonication of KGa-1 sample (from 506 to 482ºC). The different shifts can be explained in terms of differences in the reduction of particle-size.

An explanation for the variations of the mass loss in the stages of the dehydroxylation process must be complicated. Nevertheless, as pointed out by Franco *et al*. [19], the loss of some ions and water molecules formed during the ultrasound treatment, through a

prototropic mechanism, and the loss of weakly bonded hydroxyl groups of the kaolinite layers, located on the new generated surface, which are evolved with no destruction of the 7 Å structure, are the main factor controlling the mass loss in the first stage of dehydroxylation process. After the dehydroxylation of the protonated hydroxyls and the hydroxyls exposed on the external surface of the particles, the dehydroxylation of the hydroxyl groups situated between the layers begins. This process requires the interaction of two hydroxyl groups in a two-step process to form a water molecule [26]. Thus, water molecules from the dehydroxylation process have to be evolved from the material to show a mass loss in the TG curve. The evolution of water from the material is controlled by the diffusion process, which is favoured by the reduction of particle-size as indicated by the shift of the dehydroxylation endothermic effect to lower temperatures. Thus, the small shift of the dehydroxylation peak of KGa-2 compared with that of KGa-1, could indicate that the particle-size reduction of KGa-2 is smaller than that of KGa-1, as is also indicated by the XRD data.

Concluding remarks

The ultrasound treatment of kaolinite allows the reducing of its particle-size without progressive amorphization that normally occurs during traditional grinding treatments. The effect of particle-size reduction was evaluated by thermal analyses of the sonicated kaolinite. Nevertheless, we have to take into account that this treatment produces, in the well-ordered kaolinite (KGa-1), an increase in the structural disorder, which like particle-size reduction, also influences the dehydroxylation process. For this reason, it is not easy to establish the real effect of the particle-size reduction in this kind of kaolinite.

On the other hand, in this work it was shown that the only effect of the sonication in disordered kaolinite (KGa-2) is the reduction of the particle-size (Table 1), without modification in the proportion of structural disorder. Moreover, the smaller increase in specific surface area and the smaller particle-size reductions along the c^*-axis compared to that obtained with the well-ordered kaolinite (KGa-1) indicates that the disordered kaolinite offers a higher resistance to the sonication treatment.

The particle-size reduction causes the following modifications in the dehydroxylation process of kaolinite:

- An increase of the mass loss between 140 and 390ºC. The mass loss in this stage must be ascribed to the loss of the loosely bonded hydroxyl groups located on the new generated surface of the delaminated kaolinite. This mass loss increases with the increase in the specific surface area and the number of hydroxyls exposed on the external surface of particles.
- A shift to lower temperatures of the endothermic effect associated with the mass loss between 390 and 600ºC (24ºC in the well ordered kaolinite and 9ºC in the disordered sample). This shift is attributed to the size reduction of the particles improving the diffusion of the evolved water molecules compared to their diffusion in large particles.

- A decrease of the mass loss above 600ºC and a shift of the end of dehydroxylation to lower temperatures. The mass loss in this stage is related to the loss of the hydroxyl groups trapped in the metakaolinite structure [27]. The particle-size reduction has a clear effect on the temperature of the end of dehydroxylation process. The reduced particles eliminate easily the ions trapped in the metakaolinite structure because the distance that the group must travel to leave to the exterior is smaller.

The observed modifications in the dehydroxylation process of kaolinite are more pronounced in the well-crystallized sample (KGa-1). The intensity of these modifications is related to the effectiveness of the ultrasound treatment. With increasing delamination, more hydroxyls are exposed on the external surfaces and, consequently, higher mass losses between 140 and 390ºC occur. On the other hand, with decreasing particle-size higher shifts to lower temperatures of the endothermic effect between 390 and 600ºC are observed.

* * *

The authors are grateful to S. Yariv, I. Lapides and S. Shoval for carefully reviewing this paper and making helpful comments. This research has been supported by Research Project MAT 2002-03774 from the Spanish Ministry of Science and Technology and Research Groups FQM-187 and RNM-0199 of the Junta de Andalucía.

References

1 H. H. Murray, Clay Miner., 33 (1999) 65.
2 H. H. Murray, Appl. Clay Sci., 17 (2000) 207.
3 B. T. Shaw, J. Phys. Chem., 46 (1942) 1032.
4 W. D. Laws and J. B. Page, Soil Sci., 62 (1945) 319.
5 R. D. Dragsdorf, H. E. Kissinger and A. T. Perkins, Soil Sci. Soc. Am., 71 (1951) 439.
6 T. Haase and K. Winter, Bull. Soc. Fr. Ceram., 44 (1959)13.
7 J. G. Miller and T. D. Oulton, Clays Clay Miner., 18 (1970) 313.
8 Z. Juhász, Acta Mineralogica-Petrographica [suppl.], 24 (1980) 121.
9 J. Kristóf, R. L. Frost, J. T. Kloprogge, E. Horváth and É. Makó, J. Therm. Anal. Cal., 69 (2002) 77.
10 P. J. Sánchez-Soto, M. C. Jiménez de Haro, L. A. Pérez-Maqueda, I. Varona and J. L. Pérez-Rodríguez, J. Am. Ceram. Soc., 83 (2000) 1649.
11 L. A. Pérez-Maqueda, O. B. Caneo, J. P. Poyato and J. L. Pérez-Rodríguez, Phys. Chem. Minerals, 28 (2001) 61.
12 J. L. Pérez-Rodríguez, F. Carrera, J. P. Poyato and L. A. Pérez-Maqueda, Nanotechnology, 13 (2002) 382.
13 A. Pérez-Maqueda, F. Franco, M. A. Avilés, J. P. Poyato and J. L. Pérez-Rodríguez, Clays Clay Miner., (in press).
14 F. Franco, L. A. Pérez-Maqueda and J. L. Pérez-Rodríguez, Thermochim. Acta, 404 (2003) 71.
15 L. Heller-Kallai and I. Lapides, J. Therm. Anal. Cal., 71 (2003) 689.
16 F. Franco and M. D. Ruiz Cruz, J. Therm. Anal. Cal., 73 (2003) 151.
17 H. Van Olphen and J. J. Fripiat, Oxford, Pergamon 1979, p. 346.
18 S. J. Chipera and D. L. Bish, Clays Clay Miner., 49 (2001) 398.
19 S. Guggenheim and A. F. K. van Groos, Clays Clay Miner., 49 (2001) 433.

20 D. N. Hinckley, Clays Clay Miner., 11 (1963) 229.
21 B. D. Cullity, Diffraction 1: The directions of diffracted beams, In: Elements of X-ray diffrac - tion, Addison-Wesley Publishing Co., Inc., USA 1956, p. 78.
22 F. Franco, L. A. Pérez-Maqueda and J. L. Pérez-Rodríguez, J. Colloids Interface Sci., (in press).
23 K. Okada, N. Otsuka and J. Ossaka, J. Am. Ceram. Soc., 69 (1986) 51.
24 B. Sonuparlak, M. Sarikaya and I. A. Aksay, J. Am. Ceram. Soc., 70 (1987) 837.
25 P. Dion, J. F. Alcover, F. Bergaya, A. Ortega, P. L. Llewellyn and F. Rouquerol, Clay Miner., 33 (1998) 269.
26 R. L. Frost and A. M. Vassallo, Clays Clay Miner., 44 (1996) 635.
27 O. Castelein, B. Soulestin, J. P. Bonnet and P. Blanchart, Ceram. Int., 27 (2001) 517.